

FIG. 3. Raman spectrum of the  $\gamma$  phase at 8°K: (a) lattice region; (b) stretching region.

low the peak and is possibly part of the instrumental profile made visible by the extreme elastic scattering from the sample. Figure 3 also shows an asymmetrical line in the stretching region with a frequency of 2331  $\text{cm}^{-1}$ . Table V shows the results for different temperatures.

The librational frequencies calculated in the harmonic approximation including quadrupolar interactions to 12th nearest neighbors are  $\omega(E_g) = 42 \text{ cm}^{-1}$  and  $\omega(B_{1g}) = 82 \text{ cm}^{-1}$ . A calculation of the relative intensities for polarized incident light in the usual  $90^\circ$  scattering geometry yields the ratio 1.8:1 favoring the  $E_g$  mode.<sup>69</sup> On the basis of these calculations the low and high frequency Raman lines are assigned to librational modes of  $E_g$  and  $B_{1g}$  symmetry, respectively.<sup>58</sup> The poor agreement between calculated and measured frequencies is to be expected since, at the higher densities corresponding to the  $\gamma$  phase, the repulsive part of the potential becomes more important. Calculations using the 6-12<sup>38</sup> and 6-exp<sup>68</sup> atom-atom potentials are in good agreement with experiment.

The strong temperature dependence of the  $B_{1g}$  librational frequency seems to point to a softening of this mode as the  $\gamma$  to  $\beta$  transition is approached. In going to the  $\beta$  phase, where the molecular centers are arranged in an hcp structure, the square faces of the unit cell of  $\gamma\text{-N}_2$  shown in Fig. 2 have to be sheared. The  $B_{1g}$  librational mode, which corresponds to librations in the plane of the square faces, can then become soft through coup-

TABLE V. Observed Raman frequencies and relative intensities for the  $\gamma$  phase.

Temperature	Frequency ( $\text{cm}^{-1}$ )	Relative integrated intensity
35°K	57.5	2
	95.5	4.5
	2329	1
20°K	58.2	5.5
	102.5	3
	2330	1
8°K	58.4	7
	103.6	2.5
	2331	1

ling to the infrared active  $E_g$  translational mode that corresponds to the shearing motion.

### B. Volume dependence of the Raman frequencies in the $\alpha$ phase

Figure 4 shows the Raman spectrum in the lattice region of the  $\alpha$  phase. Three sharp lines are observed corresponding to librations of  $E_g$ ,  $T_{2g}$ , and  $T_{1g}$  symmetry, in agreement with previous results.<sup>19-23</sup> In addition, a broad band is observed from about 70 to 100  $\text{cm}^{-1}$ . In the stretching region, not shown in Fig. 4, two lines with a separation of about 1.2  $\text{cm}^{-1}$  have been resolved.

Samples 1-3 were grown to study the volume dependence of the Raman frequencies in the  $\alpha$  phase. The results for these samples are summarized in Table VI. Because of broadening, only the frequency of the  $E_g$  line could be determined at 33°K. The frequencies increase with decreasing molar volumes, while the full widths at half intensity seem to be independent of volume.

The lattice frequencies are independent of volume and temperature in the harmonic approximation. In the quasi-harmonic approximation<sup>70</sup> the frequencies are dependent on volume. Usually the dominant quasi-harmonic contribution to the volume dependence arises because of a shift in the point of evaluation of the second order force constants used in a harmonic calculation. A measure of the volume dependence of the normal mode frequencies  $\omega(j)$  is given by the Grüneisen parameter of the  $j$ th mode

$$\gamma_j = (-\partial \ln \omega(j) / \partial \ln V)_T, \quad (1)$$

where  $V$  is the molar volume. These parameters are critically dependent on the form of the intermolecular

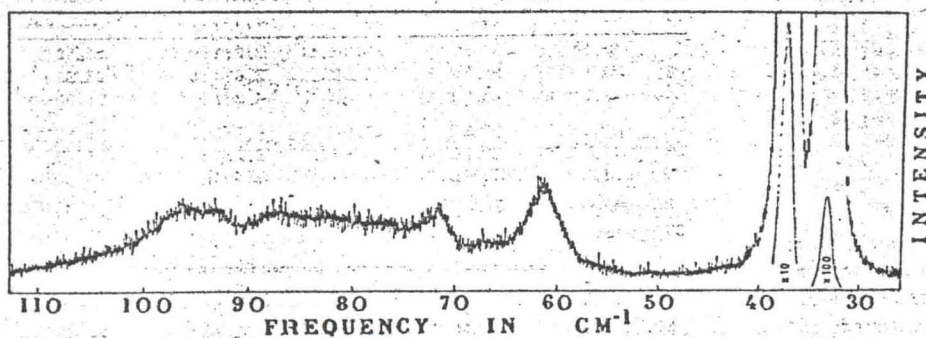


FIG. 4. Raman spectrum in the lattice region of the  $\alpha$  phase for a sample with a molar volume of 26.82  $\text{cm}^3/\text{mole}$  at 8°K. Instrumental resolution is 1  $\text{cm}^{-1}$ .